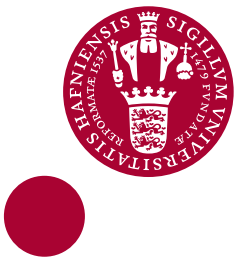

The states of water in Norway spruce (Picea abies (L.) Karst.) studied by low-field nuclear magnetic resonance (LFNMR) relaxometry

assignment of free-water populations based on quantitative wood anatomy

Fredriksson, Maria; Thygesen, Lisbeth Garbrecht

Published in:
Holzforschung

DOI:
10.1515/hf-2016-0044

Publication date:
2017

Document version
Publisher's PDF, also known as Version of record

Open Access

Maria Fredriksson* and Lisbeth Garbrecht Thygesen

The states of water in Norway spruce (*Picea abies* (L.) Karst.) studied by low-field nuclear magnetic resonance (LFNMR) relaxometry: assignment of free-water populations based on quantitative wood anatomy

DOI 10.1515/hf-2016-0044
Received February 23, 2016; accepted August 15, 2016; previously published online xx

Abstract: Low-field nuclear magnetic resonance (LFNMR) relaxometry was applied to determine the spin-spin relaxation time (T_2) of water-saturated Norway spruce (*Picea abies* (L.) Karst.) specimens cut from mature sapwood (sW) and mature and juvenile heartwood (hW), where earlywood (EW) and latewood (LW) were separated. In combination with quantitative wood anatomy data focusing on the void volumes in various morphological regions, the NMR data served for a more reliable assignment of free-water populations found in water-saturated solid wood. Two free-water populations were identified within most sample types. One was assigned to water in the tracheid lumen and the other to water inside bordered pits. Whether water in the ray cell lumina was included in one or the other of these two populations depends on the curve-fit method applied (continuous or discrete). In addition, T_2 differences between the different tissue types were studied and, for comparison, sorption isotherms were measured by means of a sorption balance. There was a significant difference between EW and LW as well as between juvenile wood and mature wood in terms of T_2 related to the cell wall water. However, no differences were seen between the sorption isotherms, which indicates that the observed T_2 differences were not due to differences in cell wall moisture content (MC).

***Corresponding author: Maria Fredriksson,** Department of Geosciences and Natural Resource Management, University of Copenhagen, Rolighedsvej 23, DK-1958 Frederiksberg C, Denmark; and Division of Building Materials, Lund University, P.O. Box 118, SE-221 00 Lund, Sweden, e-mail: maria.fredriksson@byggtek.lth.se
Lisbeth Garbrecht Thygesen: Department of Geosciences and Natural Resource Management, University of Copenhagen, Rolighedsvej 23, DK-1958 Frederiksberg C, Denmark

Keywords: dynamic vapour sorption (DVS), earlywood (EW), juvenile wood, latewood (LW), low-field nuclear magnetic resonance (LFNMR), moisture content (MC), sorption isotherm, spin-spin relaxation time (T_2)

Introduction

The moisture content (MC) as well as the location of the water, i.e. bound water in the cell wall or free water in voids such as cell lumina or bordered pits, influence wood degradation by wood-degrading fungi (Ibach 2013) as well as most physical wood properties such as strength and dimensional stability (Shmulsky and Jones 2011). Quantitative and qualitative methods for moisture characterization are consequently of high value.

Low-field nuclear magnetic resonance (LFNMR) has previously been used to study water in wood, both to determine MC (Sharp et al. 1978; Hartley et al. 1994, 1996; Merela et al. 2009) and to differentiate between different water states or populations (Menon et al. 1987, 1989; Flibotte et al. 1990; Araujo et al. 1992, 1994; Labbé et al. 2002, 2006; Almeida et al. 2007; Thygesen and Elder 2008, 2009). The LFNMR approach is decribed by Rutledge (1992). In short, the spin-spin relaxation time (T_2) determined by LFNMR is a measure of how tight the water is bound: the more tight the bonding, the shorter the T_2. Provided that the pore wall surfaces are similar throughout the material, the T_2 of the free water is related to the surface area to pore volume ratio where liquid water in smaller pores have a shorter T_2 than in larger pores (Brownstein and Tarr 1979; Menon et al. 1987; Almeida et al. 2007). The T_2 of free water is not only related to the pore-radius and pore-wall properties, but can also be influenced by the presence of solutes (Hsieh et al. 2014).

In LFNMR studies on softwoods, three or four peaks representing different water populations have been identified in water-saturated or green specimens (Menon et al. 1987, 1989; Flibotte et al. 1990; Araujo et al. 1992; Labbé et al. 2002, 2006; Thygesen and Elder 2008). The 1st peak, generally at <3 ms (Menon et al. 1987; Araujo et al. 1992, 1994; Labbé et al. 2002, 2006; Thygesen and Elder 2008; Telkki et al. 2013) is assigned to the water bound in the cell wall, while peaks with a longer T_2 are assigned to free water. This differentiation between bound water and free water is made because the former has a T_2 which is constant and independent of MC changes above the fibre saturation point (FSP) (Araujo et al. 1992). Below the FSP, however, the amplitude (Araujo et al. 1992) as well as the T_2 of this peak decreases with decreasing MC (Menon et al. 1987; Araujo et al. 1994; Almeida et al. 2007). Peaks with longer T_2 are attributed to free water, because their amplitudes decrease with decreasing MC above the FSP (Araujo et al. 1992). In addition, a 4th peak with a longer T_2 was detected in two studies (Labbé et al. 2006; Thygesen and Elder 2008). Labbé et al. (2006) attributed this peak to organic compounds.

In the studies where two peaks were found for free water, these were in the ranges 9–80 ms and 30–400 ms, respectively (Menon et al. 1987; Flibotte et al. 1990; Araujo et al. 1992; Labbé et al. 2002, 2006). As the pore size influences the T_2, the free-water peak with the shortest T_2 (9–80 ms) has been attributed to water in latewood (LW) lumen and ray cells, while the free-water peak with the longer T_2 (30–400 ms) has been attributed to water in the larger earlywood (EW) lumina (Menon et al. 1987, 1989). A shorter T_2 in LW than in EW was also observed by magnetic resonance imaging (MRI) (Javed Muhammad et al. 2015).

So far, the assignment of free-water populations within wood has been made by qualitatively sorting and pairing the observed T_2 values with the void sizes present within the specimens because water inside smaller voids generally has a shorter T_2. However, in the present study, the assignment is based on relative amplitudes/peak areas obtained from LFNMR data of Norway spruce (*Picea abies* (L.) Karst.) and the void volumes available for free water. That is, rather than relying on observed T_2 values only, the information captured by the LFNMR measurement regarding the amount of water in each of these populations was also taken into account. In addition, to reduce the number of possible void types, well-defined specimens were investigated. Furthermore, the specimens were measured both before and after extraction to identify possible effects of extractives. Finally, LFNMR data were compared with sorption isotherms determined for all wood types to study possible differences in MCs within the cell wall.

Materials and methods

Materials: Samples were taken from one Norway spruce (*Picea abies* (L.) Karst) tree from a stand in the southern part of Sweden, see Fredriksson et al. (2016) for details. Specimens were cut from a total of 30 individual growth rings of mature sapwood (sW), mature heartwood (hW) and juvenile hW, i.e. 10 growth rings of each wood type. For each wood type, specimens were taken from two different boards. EW and LW were separated; hence, a total of 60 specimens were prepared (Table 1).

All specimens were cut to 10 mm in the longitudinal direction. The cross section of each specimen was cut to fit into the NMR tube (inner diameter 8 mm) so that the vacuum-saturated mass of each specimen was about 0.15 g. Because of the thin LW rings, two LW pieces were needed to obtain approximately the same mass as one EW specimen. All specimens were vacuum-saturated in vacuum (0–1 mbar) for 1 h. Deionized water was then let in and finally atmospheric pressure was applied.

NMR: The measurements were performed on vacuum-saturated specimens. Each specimen was wiped on a wet piece of paper to avoid the presence of free water in the NMR tube, but without drying the specimen. In the case of LW, where two pieces were needed, both pieces were wiped individually to avoid free water between them. The specimens were then placed in the NMR tubes, which were sealed with a cap and placed in the NMR instrument (mq20-Minispec, Bruker, Billerica, MA, USA) with a 0.47-Tesla permanent magnet, which corresponds to a 20-MHz proton resonance frequency. Care was taken so that the specimen orientation was the same for all measurements. The spin-spin relaxation time (T_2) was determined using the Carr-Purcell-Meiboom-Gill (CPMG) pulse sequence with a pulse separation (τ) of 0.1 ms, 8000 echoes, gain 82 dB, 32 scans and a recycle delay of 5 s. The 90° and 180° radio frequency pulses in the instrument have the same radio frequency gain and hence the 180° is about twice the duration of the 90° pulse (3.54 µs and 7.22 µs, respectively). The magnet temperature was 40°C, but the probe used enabled temperature control of the sample tube by water circulation.

Table 1: The vacuum-saturated moisture content (u_{vac}) of the earlywood (EW) and latewood (LW) specimens of mature sapwood (sW), mature heartwood (hW) and juvenile hW.

	u_{vac} (kg kg^{-1})	No. of specimens	
		LFNMR	Sorption isotherms
Mature sW			
EW	2.83	10	2
LW	1.3	10	2
Mature sW			
EW	2.94	10	2
LW	1.29	10	2
Juvenile hW			
EW	2.95	10	2
LW	1.65	10	2

The number of specimens in each group included in the LFNMR measurements and the sorption isotherm measurements, respectively, is also shown.

The sample temperature was set to 20°C. As the room temperature was 23°C, the specimen was kept in the NMR for 5 min before the measurement started. The mass of each specimen was determined before each NMR measurement.

After the measurements, the specimens were dried, first above water in a desiccator (i.e. close to 100% relative humidity, RH) for 4 weeks and then at 45°C for 19 days. Hereafter, the equilibrium mass at 45°C was determined. Half of the specimens were then extracted in ethanol for 24 h in a Soxhlet apparatus. These specimens were then again dried at 45°C for 8 weeks and their mass was determined. The extracted specimens were then vacuum-saturated by the procedure described above, and a second set of NMR measurements was performed. Finally, all specimens were dried at 105°C for 24 h, the dry mass (m_{dry}) was determined and the MC (u) was calculated as:

$$u = \frac{m_{eq} - m_{dry}}{m_{dry}} \quad (1)$$

where m_{eq} is the mass of the vacuum-saturated specimens. For the extracted specimens, the dry mass was adjusted in order to calculate the MC on the same terms as for the non-extracted specimens. The mass of the extractives (m_{extr}) was determined as:

$$m_{extr} = m_{1,45°C} - m_{2,45°C} \quad (2)$$

where $m_{1,45°C}$ is the equilibrium mass at 45°C before extraction and $m_{2,45°C}$ is the equilibrium mass at 45°C after extraction. The dry mass of the extracted samples was determined by adding the mass of the extractives m_{extr} to the dry mass of the extracted specimen determined at 105°C. The average extractive content in relation to the dry mass was about 2%, which is in agreement with literature data for *P. abies* (Fengel and Wegener 2003). The average MC after vacuum saturation for each group of specimens is given in Table 1.

Data evaluation: The CPMG data were normalized by dividing the relative intensity by the vacuum-saturated mass of each specimen. These data were then evaluated using two methods: discrete multi-exponential fitting (Pedersen et al. 2002) and the Laplacian transformation method Contin as described by Provencher (1982). For the discrete multi-exponential fitting the CPMG data were fitted to:

$$y = C_1 e^{-\frac{t}{T_{2,1}}} + \ldots + C_n e^{-\frac{t}{T_{2,n}}} + C_{n+1} \quad (3)$$

based on up to five components. Four components were chosen because there was only a minor decrease in the residual sum of squares when an additional component was added. The Contin method gives a continuous distribution of the relaxation times (T_2) for each specimen, 256 data points were used in the 0.01–10 000 ms range. From this continuous distribution, the T_2 value corresponding to the maximum amplitude of each peak was determined. Here, five peaks were identified, but all peaks were not present for all specimens. The T_2 values for the different peaks for both the multi-exponential and the Contin fit were analysed by analysis of variance (ANOVA) to establish differences between the different groups of specimens (EW/LW, mature/juvenile wood, hW/sW) and the influence of extraction. For ANOVA, the Statistics Toolbox in MATLAB (MATLAB R2013b, The MathWorks, Inc., Natick, MA, USA) was used. In addition, the relative amplitudes (multi-exponential fit) and the relative area under each peak (Contin) were evaluated. The latter was evaluated as $dS/d(\ln T_2)$ (Terenzi et al. 2015).

Volume estimation of spaces in the wood structure available for free water: The amplitude of each T_2 component represents the relative amount of water (McDonald et al. 2010) and for a continuous curve-fit, the area under the curve is proportional to the amount of water (Labbé et al. 2006). To clarify which water the two peaks related to free water represent, the volumes of all spaces in the wood structure that contain free water were determined. Dimensions of the lumen cross section of mature EW and LW were estimated based on images taken with a scanning electron microscope (SEM, SU3500, Hitachi High-Technologies Corporation, Krefeld, Germany). The specimens were prepared by cutting thin slices with a razor blade, mounting them on sample holders and finally sputter coating the samples with gold (Cressington 108 Auto Sputter Coater, Cressington Scientific Instruments Ltd., Watford, UK). The other dimensions and parameters are based on literature data as presented in Table 2. The void volumes available for free water were calculated with the Eqs. (4–21); all parameters in these equations are defined in Figure 1.

The volume of the tracheid lumen, V_{lumen}, was determined by assuming a rectangular cross section:

$$V_{lumen} = d_1 d_2 (l_{trach} - 2(h_{end} + t_{cw})) \quad (4)$$

As the tracheid ends are tapered, the volume of the tracheid ends was determined separately as:

$$V_{end} = \frac{d_1 d_2 h_{end}}{2} \quad (5)$$

The volume of the pit chamber was assumed to be the same irrespective of whether the pit was aspirated or not. The volume was determined as twice the volume of a spherical cap:

$$V_{pit} = 2 \cdot \frac{\pi h_{pit}}{6} \left(3 \left(\frac{d_{pit}}{2} \right)^2 + h_{pit}^{\ 2} \right) \quad (6)$$

As the cell walls of LW are thicker, the aperture of the bordered pits resembles a capillary rather than an orifice (Siau 1984); it is thus possible that water is held here. The aperture was approximated to be cylindrical and the volume was calculated:

$$V_{ap} = \pi \left(\frac{h_{ap}}{2} \right)^2 t_{cw} \quad (7)$$

Norway spruce contains both parenchymatous and tracheidal ray cells (Back 1958). Both the length (Back 1958) and the types of pits (Nyrén and Back 1960) differ between these two cell types, and they were therefore considered separately in the volume calculations. The lumen of the ray cells was determined by assuming a rectangular cross section:

$$V_{lumen,\,rays} = a_1 a_2 l_{ray} \quad (8)$$

where l_{ray} is the length of the tracheidal ($l_{ray,\,rt}$) and parenchymatous ($l_{ray,\,rp}$) ray cells, respectively. The volume of the simple pits, $V_{pit,\,rp}$, connecting the parenchymatous ray cells was determined by:

$$V_{pit,\,rp} = 2 t_{cw,\,ray} \pi \left(\frac{d_{pit}}{2} \right)^2 \quad (9)$$

The volume of the pit chamber of the bordered pits connecting the tracheidal ray cells, $V_{pit,\,rt}$, was determined as for the bordered pits in the tracheids by Eq. (6). In the literature, relative volumes of tracheid cells and ray cells can be found. However, as the numbers of bordered

Table 2: Dimensions used for determination of void volumes available for free water (see Figure 1 for definitions of the parameters).

Cell type and parameters	Mature wood				Juvenile wood			
	EW		LW		EW		LW	
	Mean	(Min/max)	Mean	(Min/max)	Mean	(Min/max)	Mean	(Min/max)
Tracheid cells								
d_1 (μm)	38[a]	(26/58)[a]	15[a]	(10/25)[a]	28.5[j]	(20/44)[j]	11.3[j]	(8/19)[j]
d_2 (μm)	30[a]	(26/58)[a]	12[a]	(10/25)[a]	22.5[j]	(20/44)[j]	9[j]	(8/19)[j]
t_{cw} (μm)	1[a]		5[a]		0.8[j]		3.8[j]	
h_{end} (μm)	80[b]	(50/110)	80[b]	(50/110)	80[b]	(50/110)	80[b]	(50/110)
l_{trach} (μm)	2836[d]	(2016/2432)[d]	3545[c]	(2520/4290)[c]	1592[d]	(832/2160)[d]	1990[c]	(1040/2700)[c]
r_{pit} (μm)	9.3[e]		2.5[e]		9.3[e]		2.5[e]	
h_{pit} (μm)	1.3[f]		6.5[f]		1.0[f]		4.9[f]	
h_{ap} (μm)	–		2.1[e]		–		2.1[e]	
n_p	200[i]		30[i]		200[i]		30[i]	
	Parenchymatous		Tracheidal					
	Mean	(Min/max)	Mean	(Min/max)				
Ray cells								
l_{ray} (μm)	175[h]	(80/325)[h]	75[h]	(30/200)[h]				
d_{pit} (μm)	1.75[g]		9[g]					
$h_{pit, rt}$ (μm)			2.6[f]					
n_p	126[k]		54[k]					
	Parenchymatous and tracheidal							
a_1 (μm)	9[a]		(5/15)[a]					
a_2 (μm)	15[a]		(10/20)[a]					
$t_{cw, ray}$ (μm)	2[g]							
p_r	0.062[h,i]							
p_{rt}	0.37[g]							
p_{rp}	0.63[g]							

The mean values were used to determine the volumes in Table 5 and Figure 5 and the minimum and maximum values were used to calculate how much some individual wood parameters influenced the calculated volumes (Figure 2). [a]SEM; [b](Engelund et al. 2010); [c](Brändström 2001); [d]80% of the LW tracheid length, as EW tracheids are shorter (Brändström 2001); [e]average for *Picea sitchensis* (Bong.) Carr. and *Picea orientalis* (L.) Link. (Usta and Hale 2006); [f]set to 1.3 times the cell wall thickness; [g](Nyrén and Back 1960); [h](Back 1958); [i](Ilvessalo-Pfäffli 1995); [j]75% of the width of mature cells (Boutelje 1968); [k]10–25 pits/100 μm cell wall length (Nyrén and Back 1960).

pits and tracheid ends depend on the number of cells, the numbers of tracheid cells and ray cells were estimated. The volume of one ray cell (including the cell wall) was estimated by:

$$V_{ray} = (a_1 + 2t_{cw, ray})(a_2 + 2t_{cw, ray})l_{ray} \quad (10)$$

The number of ray cells was then estimated by:

$$n_r = \frac{p_r}{V_{ray}} \quad (11)$$

where p_r is the relative volume of ray cells. The volume of one EW and LW cell, respectively, was estimated by:

$$V_{trach} = (d_1 + 2t_{cw})(d_2 + 2t_{cw})l_{trach} \quad (12)$$

The number of tracheids in the EW and LW, respectively, could then be estimated as:

$$n_t = \frac{1 - p_{ray}}{V_{trach}} \quad (13)$$

The total volumes of the tracheid lumen $V_{tot, lumen,}$ the tracheid lumen ends $V_{tot, ends}$, the bordered pits $V_{tot, pit}$, the apertures of the bordered pits in the LW $V_{tot, ap}$, the tracheidal ray cell lumina $V_{tot, lumen, rt}$, the parenchymatuous ray cell lumina $V_{tot, lumen, rp}$, the pits in the tracheidal ray cells $V_{tot, pit, rt}$ and the pits in the parenchymatous ray cells $V_{tot, pit, rp}$ were finally estimated for EW and LW, respectively, as:

$$V_{tot, lumen} = n_t V_{lumen} \quad (14)$$

$$V_{tot, ends} = n_t 2V_{end} \quad (15)$$

$$V_{tot, pit} = n_t n_p V_{pit} \quad (16)$$

$$V_{tot, ap} = n_t n_p V_{or} \quad (17)$$

$$V_{tot, lumen, rt} = n_r p_{rt} V_{r,rt} \quad (18)$$

$$V_{tot, pit, rt} = n_r p_{rt} V_{pit, rt} \quad (19)$$

$$V_{tot, lumen, rp} = n_r p_{rp} V_{r, p} \quad (20)$$

$$V_{tot, pit, rp} = n_r p_{rp} V_{pit, rp} \quad (21)$$

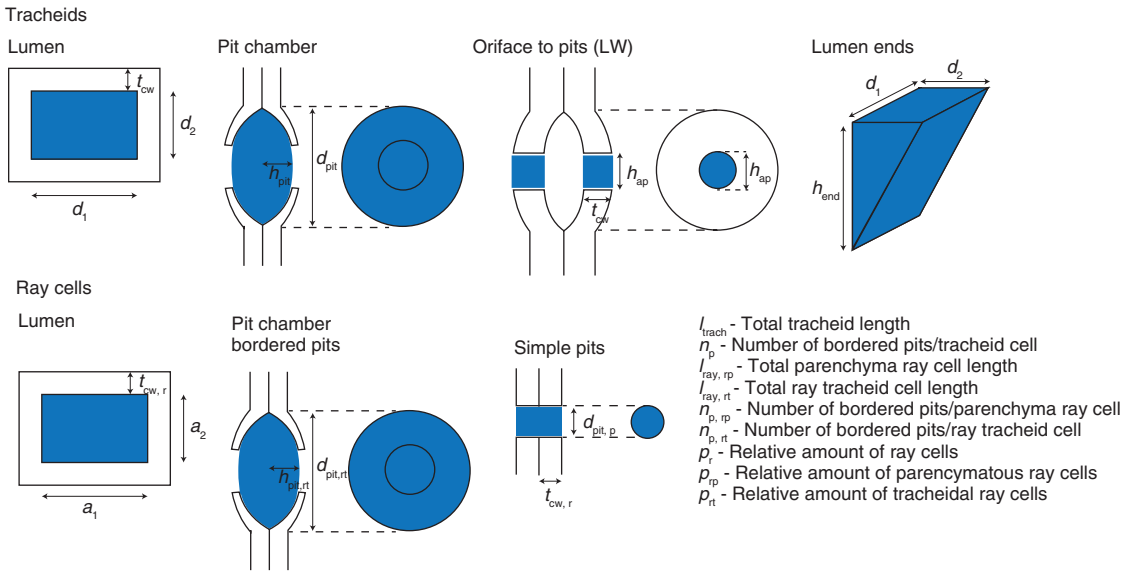

Figure 1: Definition of all parameters used in Eqs. (4–21) for determination of the void volumes in the wood structure available for free water.

The relative volumes were estimated by dividing the volume of each space by the total volume, i.e. the sum of Eqs. (14–21).

Initially, all volumes were estimated based on the mean values given in Table 2. However, the width and the length of the tracheid and the ray cells as well as the size of h_{end} were also varied between the minimum and maximum (Table 2) to get an idea of how much the individual dimensions influence the results. The parameters were varied one at a time.

Sorption isotherms: Measurements were performed in a sorption balance (dynamic vapour sorption, DVS Advantage, Surface Measurement Systems Ltd., London, UK). Here, the RH is regulated by changing the proportions of dry and water-saturated nitrogen gas. The sorption balance monitors the mass of the specimen with a resolution of 0.1 µg while the relative humidity is incrementally changed. The method is further described by Williams (1995). Small specimens were cut from the vacuum-saturated specimens prepared for the NMR measurements. For water removal from the specimen surface, the specimen was wiped by a moist cloth before it was placed in the sorption balance. The specimens were equilibrated to the following RH-levels: 97, 95, 90, 85, 80, 70, 60, 50, 40, 20, 10, 5 and 0%. The RH was then increased again in the same steps. The measurements were performed at 20°C and the equilibrium criterion (dm/dt) was set to 0.001% min^{-1} over a 10-min period. The dry mass of each specimen was 4–10 mg.

Results and discussion

Volumes in the wood structure available for free water

The void volumes in the wood structure available for free water estimated based on the mean values in Table 2 are shown in Table 3. In addition, one parameter at a time was varied between the minimum and maximum values (Table 2) to understand the influence of individual parameters. In Figure 2 it is seen that the tracheid length and width had the largest influence on the relative volumes. For LW, also the ray cell dimensions had an influence.

Sorption isotherms

The results of the sorption balance measurements (Figure 3) show that the sorption isotherms are similar for the different wood types. However, as reported in previous studies (Hill et al. 2011; Sharratt et al. 2011), small differences were seen at high RH-levels. In the present study, it

Table 3: Relative void volumes available for free water within mature wood and juvenile wood, respectively.

	Mature wood		Juvenile wood	
Cell and void type	**EW**	**LW**	**EW**	**LW**
Tracheids				
Lumen (%)	89.72	82.00	84.73	78.64
Lumen ends (%)	2.68	1.94	4.74	3.45
Bordered pits (%)	2.09	1.68	4.91	2.77
Aperture, LW pits (%)		0.07		0.22
Ray cells				
Lumen (parenchyma) (%)	2.67	6.95	2.73	7.25
Lumen (tracheids) (%)	1.57	4.08	1.60	4.26
Simple pits (%)	0.14	0.36	0.14	0.37
Bordered pits (%)	1.12	2.92	1.15	3.04

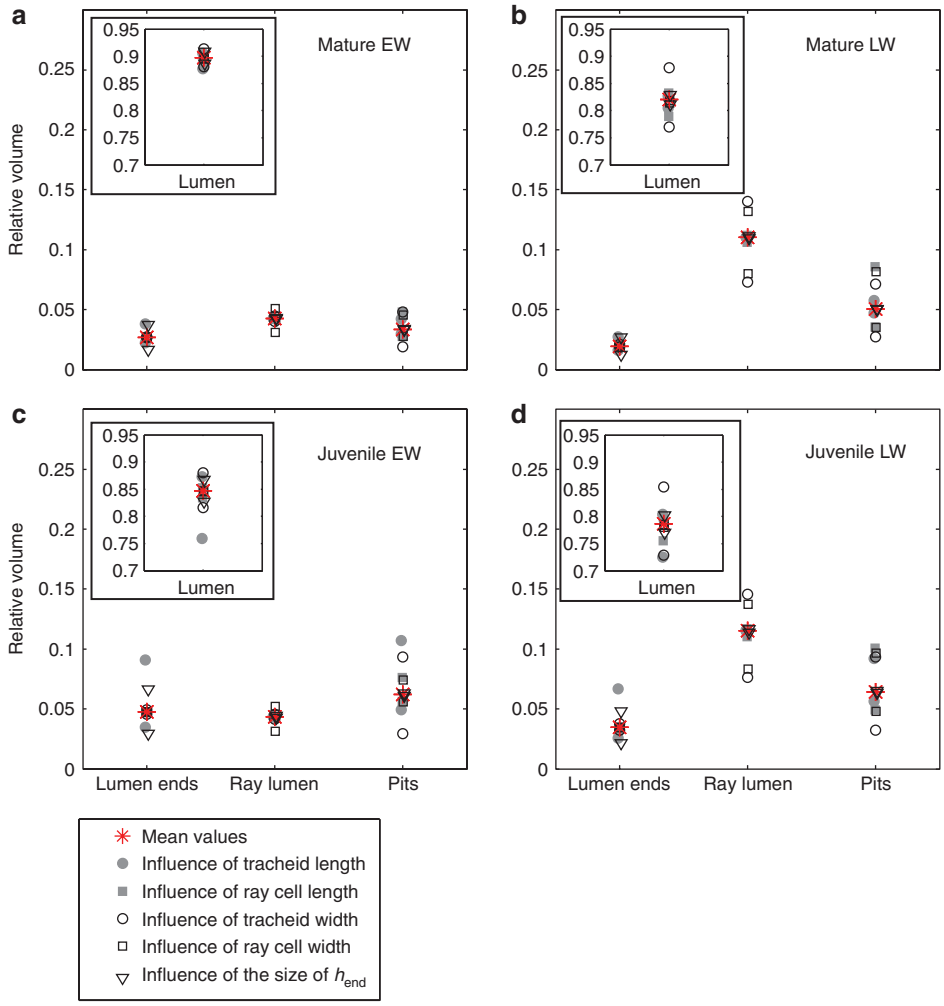

Figure 2: The influence of the tracheid and ray cell length and width as well as the influence of the size of h_{end} on the volumes available for free water for mature earlywood (EW) (a), mature latewood (LW) (b), juvenile earlywood (EW) (c) and juvenile latewood (LW) (d). The asterisk represents the relative volume determined by the mean values in Table 2. The influence of individual parameters on the volumes (squares, circles and triangles) was determined using the min and max values given in Table 2.

is not possible to ascribe these small differences to actual differences of the moisture sorption properties of the wood. Instead, it is likely that these differences are due to methodical aspects. As in most other DVS-studies, the dm/dt-criterion was the basis for equilibrium determination at each RH-level. As dm (%) is determined with the initial mass as a reference, the dm/dt-criterion does not work equally well at all RH-levels. When plotting mass as a function of time it was seen that the sample is not perfectly equilibrated at higher RH-levels.

LFNMR studies

The continuous T_2 distributions are shown in Figure 4, where the filled grey range represents the mean values with the StDs and the bars represent the components of the discrete multi-exponential fit. The relative amplitudes of the latter and the relative areas under the different peaks according to the Contin method are listed in Table 4, while the corresponding T_2 values for each peak are shown in Table 5. In general, both curve-fit methods gave the same results in terms of T_2 for the different peaks; the maxima of the continuous distribution coincided with the mean T_2 for the discrete components for Peaks 1 and 3. However, for Peaks 2 and 4 deviations were seen; the T_2 for Peaks 2 and Peak 4 were generally shorter and longer for the continuous distribution, respectively (Figure 4, Table 5).

The P-values from the ANOVA are presented in Table 6. There were significant differences between EW and LW for Peaks 1, 2 and 3, and between mature and juvenile wood for Peaks 1 and 3. No significant differences were seen

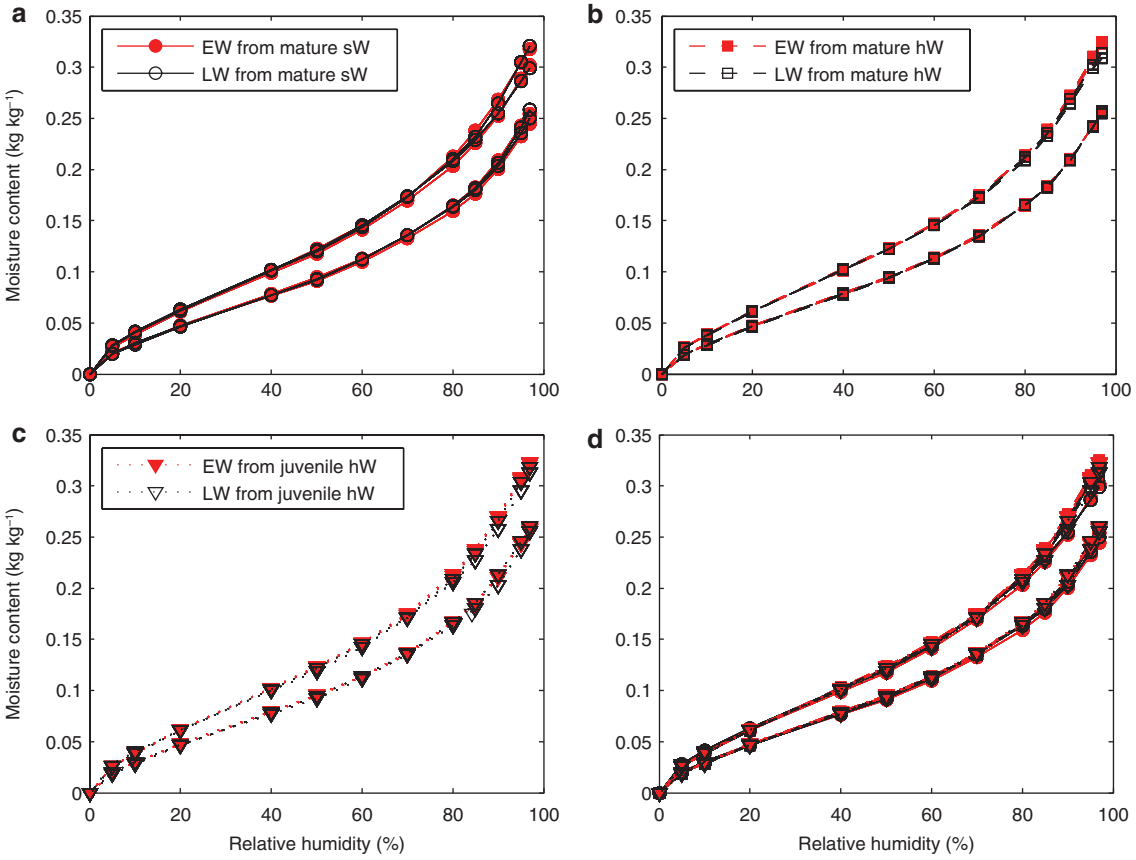

Figure 3: The sorption isotherms for earlywood (EW) and latewood (LW) of mature sapwood (sW) (a) and mature (b) and juvenile heartwood (hW) (c). All data from a, b and c are shown together in d, for legend see a–c.
Note that two replicates were used for each wood type, which is not seen in the figures since the spread was very small.

between hW and sW. Regarding the influence of extraction, the T_2 of Peak 1 was generally slightly longer and the T_2 of Peak 3 was generally slightly shorter for the extracted specimens. These differences were, however, only significant for one of the curve-fit methods (Table 6). Otherwise, the same significant differences between groups were generally seen, irrespective of the curve-fit method (continuous distribution or the discrete components).

Water populations of Peak 0

Peak 0 appeared seemingly at random, and only for a few samples (Tables 4 and 5), and it is therefore considered as an artefact.

Water populations of Peak 1

The T_2 value of Peak 1 (Table 5) was similar to the T_2 value that was ascribed to cell wall water in previous studies (Menon et al. 1987; Araujo et al. 1992, 1994; Labbé et al. 2002, 2006; Thygesen and Elder 2008; Telkki et al. 2013). A significant difference was seen between mature and juvenile wood as well as between EW and LW (Table 6). The T_2 corresponding to the cell wall water generally decreases with decreasing MC below FSP (Menon et al. 1987; Araujo et al. 1994; Almeida et al. 2007). Therefore, one explanation to the shorter T_2 for the EW compared to LW and juvenile wood compared to mature wood could be that the MC was lower in the EW and the juvenile wood cell wall. However, the results from the sorption isotherm measurements (Figure 3) performed below the FSP showed no major differences in MCs based on dry mass between the different groups. The shorter T_2 for the EW and juvenile wood could also imply that water is more tightly bound in the EW than in the LW and more tightly bound in juvenile than in mature wood. Differences in chemical composition could be one of the explanations. EW generally contains more lignin (Browning 1963; Fukazawa and Imagawa 1981; Khattak and Mahmood 1986; Gindl 2001; Bertaud and Holmbom 2004), less or a similar amount of cellulose

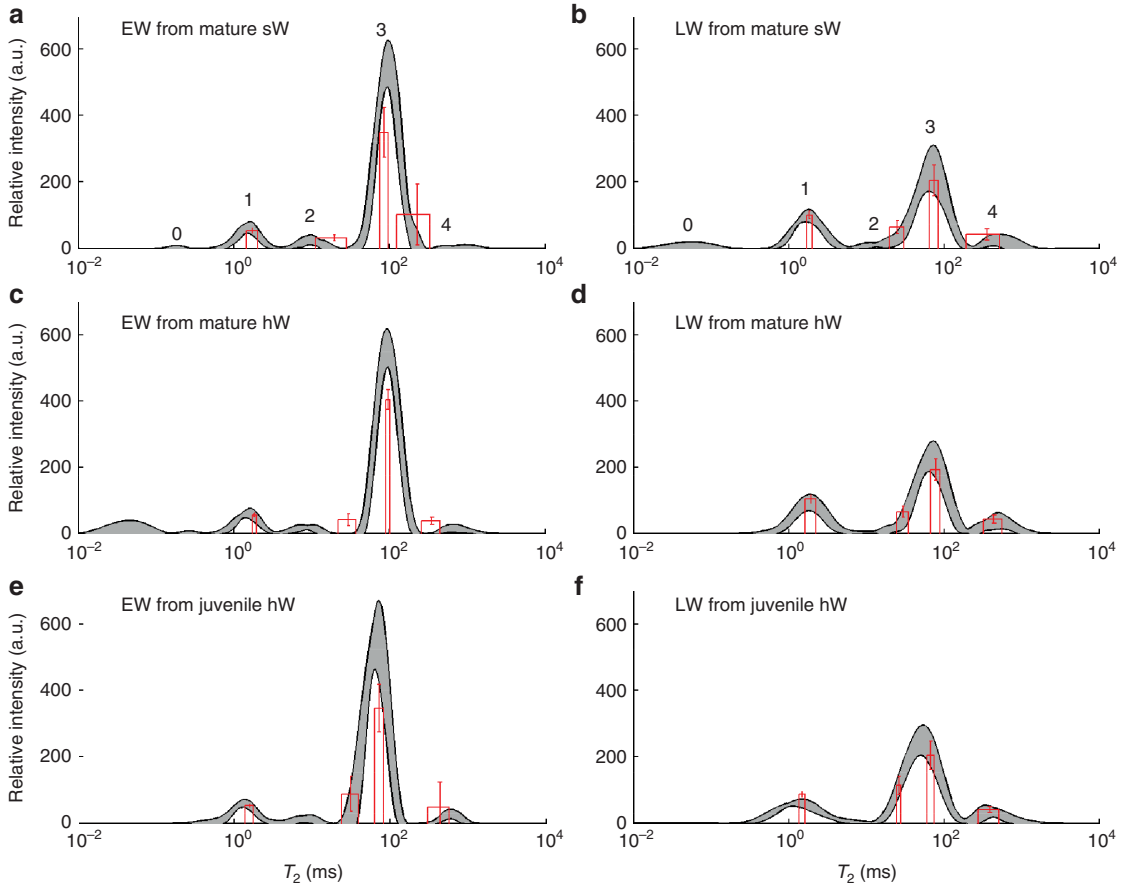

Figure 4: The continuous T_2 distribution and the fit to four discrete components (bars) are shown for earlywood (EW) (a, c, e) and latewood (LW) (b, d, f) of mature sapwood (sW) and mature and juvenile heartwood (hW).
The width of the bars and the filled area of the continuous distribution represent the mean value including the Std. The error bars on the discrete components show the Std of each amplitude. The error bar is placed at the mean T_2. The numbers in a and b refer to the numbering of the peaks used in the present study.

(Meier 1962; Browning 1963; Khattak and Mahmood 1986), and less hemicelluloses (Bertaud and Holmbom 2004) with different constituents (Meier 1962; Timell 1965; Bertaud and Holmbom 2004; Rowell et al. 2013). Elder and Houtman (2013) found that removal of hemicelluloses gave a longer T_2 for the bound water. The lower hemicelluloses content in the EW should thus give a longer T_2 and not a shorter one, which was the case in the present study. Another possible explanation for the difference between EW and LW could be that the former contains more extractives (Bertaud and Holmbom 2004). For the discrete multi-exponential fit, where extractives had a significant effect (Table 6), this interpretation fits the observation that the T_2 was generally longer for EW after extraction (Table 5). However, for the continuous curve-fit, this effect was not significant (Table 6) and the T_2 was shorter for EW also for the extracted specimens (Table 5).

Comparing juvenile and mature wood, the former contains more lignin (Harwood 1971; Uprichard 1971; Garcia Esteban et al. 2015), less cellulose (Harwood 1971; Uprichard 1971; Shupe et al. 1997; Garcia Esteban et al. 2015) and more (Garcia Esteban et al. 2015) or a similar amount of hemicelluloses (Bertaud and Holmbom 2004; Kaakinen et al. 2007). Thus, EW and juvenile wood contain more lignin than LW and mature wood, respectively, but it is not clear how this fact relates to the shorter T_2 because lignin is the least hygroscopic component in the cell wall (Siau 1984). In summary, the differences in T_2 values of the cell wall water observed between the wood types cannot be interpreted for the time being.

Water populations of Peak 4

In a previous study (Labbé et al. 2006), a T_2 value observed in a similar range as the T_2 value for Peak 4 in the present study was assigned to organic components. However, in the present study, Peak 4 was also present for

Table 4: The mean relative amplitudes (discrete multi-exponential fit) and the relative areas under each peak (continuous fit).

	Peak 0	Peak 1	Peak 2	Peak 3	Peak 4
Discrete multi-exponenital fit					
Non-extracted					
Mature sW					
EW		0.10	0.06	0.65	0.19
LW		0.25	0.16	0.50	0.10
Mature hW					
EW		0.10	0.08	0.75	0.07
LW		0.26	0.16	0.48	0.11
Juvenile hW					
EW		0.10	0.16	0.65	0.09
LW		0.20	0.25	0.46	0.09
Extracted					
Mature sW					
EW		0.10	0.09	0.74	0.07
LW		0.28	0.18	0.44	0.10
Mature hW					
EW		0.10	0.09	0.75	0.06
LW		0.29	0.17	0.47	0.08
Juvenile hW					
EW		0.10	0.12	0.75	0.03
LW		0.22	0.22	0.50	0.06
Continuous fit					
Non-extracted					
Mature sW					
EW	0.00 (3/10)	0.10	0.04 (10/10)	0.85	0.02 (8/10)
LW	0.02 (1/10)	0.25	0.02 (7/10)	0.65	0.06 (10/10)
Mature hW					
EW	0.03 (3/10)	0.09	0.03 (10/10)	0.83	0.02 (10/10)
LW	0.00 (0/10)	0.27	0.01 (6/10)	0.63	0.09 (10/10)
Juvenile hW					
EW	0.00 (0/10)	0.10	0.02 (9/10)	0.85	0.03 (9/10)
LW	0.00 (1/10)	0.21	0.01 (2/10)	0.70	0.08 (10/10)
Extracted					
Mature sW					
EW	0.01 (2/5)	0.09	0.04 (5/5)	0.83	0.02 (5/5)
LW	0.00 (0/5)	0.29	0.03 (3/5)	0.59	0.10 (5/5)
Mature hW					
EW	0.00 (2/5)	0.09	0.03 (5/5)	0.85	0.02 (5/5)
LW	0.00 (0/5)	0.31	0.00 (1/5)	0.64	0.06 (5/5)
Juvenile hW					
EW	0.00 (0/5)	0.09	0.03 (5/5)	0.86	0.01 (5/5)
LW	0.00 (0/5)	0.25	0.00 (1/5)	0.72	0.03 (5/5)

The relative amplitudes/areas were determined as the amplitude/area for each peak divided by the total amplitude/area. For the continuous curve-fit, Peaks 0, 2 and 4 did not occur for all specimens. For these peaks, the data in brackets mean the number of specimens for which this peak occurred in relation to the total number of specimens.

the extracted specimens. The influence of water on Peak 4 was investigated in a separate experiment. Specimens from four growth rings were cut into two pieces. One of the pieces was then wiped with wet paper before the NMR measurements (as was done in the actual experiment) and the other piece was wiped with dry paper. In the latter case, the 4th peak disappeared in the continuous curve-fit. For the fit to discrete components, four components gave the best fit for the specimens dried with wet paper and three components gave the best fit for the samples dried with dry paper. This indicates that Peak 4 represents surface water on the specimen. However, dry paper not only removes surface water, but also dries the actual specimen which leads to additional changes in the NMR

Table 5: Mean values of the T_2 (ms) determined by fitting to four discrete components and by a continuous curve-fit.

	Peak 0			Peak 1		Peak 2			Peak 3		Peak 4		
	mean	std		mean	std	mean	std		mean	std	mean	std	
Discrete multi-exponenital fit													
Non-extracted													
Mature sW													
EW				1.7	0.3	19.6	8.4		85.2	10.3	226.7	102.9	
LW				1.9	0.1	25.1	5.2		74.4	9.9	357.7	162.7	
Mature hW													
EW				1.8	0.1	29.6	7.7		95.4	5.6	350.0	92.7	
LW				1.9	0.3	29.7	5.2		78.1	10.5	438.6	116.5	
Juvenile hW													
EW				1.6	0.2	31.4	7.6		72.0	9.5	436.6	133.8	
LW				1.5	0.1	26.3	1.8		67.5	6.7	391.7	117.7	
Extracted													
Mature sW													
EW				2.0	0.4	27.3	10.1		91.9	8.9	374.3	137.0	
LW				1.8	0.1	24.8	3.0		71.5	10.3	508.5	33.4	
Mature hW													
EW				2.0	0.3	29.9	6.3		93.5	5.6	350.8	95.8	
LW				1.9	0.2	26.1	2.7		69.6	8.5	346.1	150.1	
Juvenile hW													
EW				1.8	0.0	26.4	4.5		72.5	5.7	307.9	55.7	
LW				1.7	0.4	21.8	2.5		60.2	3.9	278.4	82.0	
Continious fit													
Non-extracted													
Mature sW													
EW	0.3	0.1	(3/10)	1.5	0.1	9.7	2.2	(10/10)	94.1	9.7	1143.5	1279.9	(8/10)
LW	0.1	0.0	(1/10)	1.7	0.1	13.6	4.4	(7/10)	67.1	8.0	1000.9	1696.7	(10/10)
Mature hW													
EW	0.2	0.1	(3/10)	1.5	0.2	8.3	2.1	(10/10)	93.5	7.9	730.8	202.5	(10/10)
LW	–	–	(0/10)	1.9	0.3	13.8	4.4	(6/10)	67.8	9.6	491.5	150.8	(10/10)
Juvenile hW													
EW	–	–	(0/10)	1.3	0.2	8.1	2.0	(9/10)	66.5	8.9	599.5	86.3	(9/10)
LW	0.0	0.0	(1/10)	1.2	0.2	7.7	2.9	(2/10)	51.4	6.0	443.7	120.3	(10/10)
Extracted													
Mature sW													
EW	0.2	0.2	(2/5)	1.5	0.2	9.4	1.6	(5/5)	90.8	4.1	727.5	215.4	(5/5)
LW	–	–	(0/5)	1.7	0.1	14.2	4.9	(3/5)	60.9	10.8	545.2	65.1	(5/5)
Mature hW													
EW	0.1	0.0	(2/5)	1.6	0.3	9.2	0.9	(5/5)	90.9	7.2	1469.4	1665.2	(5/5)
LW	–	–	(0/5)	1.8	0.2	9.7	0.0	(1/5)	59.6	5.6	430.5	184.8	(5/5)
Juvenile hW													
EW	–	–	(0/5)	1.4	0.1	8.0	2.1	(5/5)	68.8	7.7	719.8	273.8	(5/5)
LW	0.1	0.0	(0/5)	1.7	0.4	9.7	0.0	(1/5)	48.8	7.1	402.5	192.2	(5/5)

For the continuous curve-fit, Peaks 0, 2 and 4 did not occur for all specimens. For these peaks, the number of specimens for which this peak occurred in relation to the total number of specimens is given in brackets.

data. Wiping with dry paper is thus not recommendable for water-saturated specimens.

Water populations of Peaks 2 and 3

The T_2 corresponding to Peak 3 (Table 5) is in the range that was previously assigned to lumen water in the tracheid cells (Menon et al. 1987; Araujo et al. 1992; Labbé et al. 2002, 2006; Thygesen and Elder 2008). In the present study, there was a significant difference in T_2 between EW, LW, juvenile and mature wood (Table 6). The T_2 of Peak 3 was shorter for LW, which is in agreement with previous studies (Menon et al. 1987, 1989; Javed Muhammad et al. 2015) and is due to the fact that LW lumina are smaller than those of EW. The T_2 of Peak 3 was also shorter for juvenile

Table 6: The P-values from ANOVA calculated for T_2 values from the continuous curve-fit (cont) and the discrete multi-exponential fit (exp), respectively.

		ANOVA P-values			
Factors	**Curve-fit**	**Peak 1**	**Peak 2**	**Peak 3**	**Peak 4**
hW/sW	Cont	0.333	0.254	0.947	0.370
	Exp	0.408	0.684	0.635	1.000
Mature/juvenile wood	Cont	0.000[a]	0.124	0.000[a]	0.378
	Exp	0.000[a]	0.827	0.000[a]	0.225
EW/LW	Cont	0.000[a]	0.000[a]	0.000[a]	0.106
	Exp	0.009[a]	0.001[a]	0.000[a]	0.322
Non-extr./extr.	Cont	0.035[a]	0.998	0.071	0.914
	Exp	0.057	0.250	0.011[a]	0.483

The data with [a] designate significant differences ($P < 0.05$).

than for mature wood (Table 5), which is in agreement with results of Araujo et al. (1992). This is probably due to the smaller diameters in juvenile tracheids (Brändström 2001; Schweingruber 2007).

Peak 2 has previously been assigned to water in LW lumen and rays (Menon et al. 1987, 1989), but in the present study, where LW and EW were observed separately, this peak was seen for both the EW and the LW specimens. However, Peak 2 was not always seen for the LW specimens using the continuous curve-fit (Table 5), probably because it merged with Peak 3, which could happen as the T_2 of Peak 2 was longer and the T_2 of Peak 3 was shorter in LW.

To determine the fraction of each of the two free-water peaks, the amplitudes of Peaks 2 and 3 respectively from the discrete exponential fit was divided by the sum of the amplitudes of these peaks. Similarly, the area under Peaks 2 and 3 for the continuous curve-fit was divided by the sum of the areas of Peaks 2 and 3. The results represent the relative amount of free water represented by these peaks. In Figure 5, these relative amplitudes and areas representing Peaks 2 and 3 from the LFNMR measurements are compared with the volumes available for free water in the wood structure according to the estimates given in Table 3. Note that in Figure 5, the ray cell lumen volumes and the pit volumes were summed, i.e. the ray cell lumen is the total volume of the lumina for the two ray cell types and the pit volume is the sum of all volumes related to the pits in both the tracheid cells and the ray cells. For the discrete exponential fit for the EW, the relative amplitude of Peak 3 corresponded fairly well with the relative volume of the tracheid lumen (Figure 5). Thus, the relative amplitude of Peak 2 corresponds with the volume of smaller voids (ray cell lumen, pits and tracheid lumen ends) (Figure 5). However, for LW, especially for juvenile LW, the estimated lumen volume was larger than the relative amplitude of Peak 3. Here, a better correlation with the relative amplitude of Peak 3 would be obtained in case of decreasing tracheid width or the tracheid length (Figure 2). It is not obvious why the ray cell water should be included in Peak 2 for the LW; the length of the cells is different, but the width and their surface area to pore volume ratios are similar, and thus the T_2 values are also expected to be similar. One hypothesis is that organic substances in the ray cell lumina lower the T_2. If it is true, this effect should not be seen for the extracted specimens, but the results were similar also after extraction. Another possible explanation is that the ray cells are oriented perpendicular to the tracheid cells. For the cell wall water,

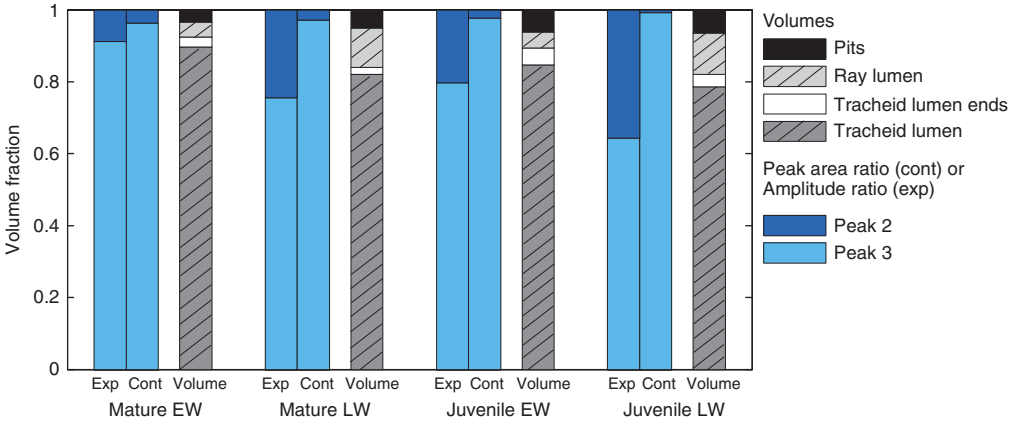

Figure 5: The volume bars represent the estimated volume fractions available for free water.
The relative amplitudes from the discrete exponential fit (exp) and the relative areas under the continuous curve-fit (cont) for the free-water peaks (Peaks 2 and 3) are also shown and show the relative amount of free water represented by Peaks 2 and 3, respectively. For mature wood, the values are average values for mature sW and hW. All LFNMR data are from non-extracted wood samples.

the orientation of the wood sample during measurement has been shown to influence ^{1}H NMR data (Terenzi et al. 2013). However, irrespective of how the dimensions are varied between the minimum and maximum values in Table 2, it is not possible to assign the ray cell lumen water to Peak 3 (Figures 2 and 5).

For the continuous curve-fit, the results were different; here the relative area under Peak 2 was small, especially for the LW, and only the water in the pits seemed to be included (Figure 5). For juvenile wood, the relative area for Peak 2 was even smaller than the volume fraction corresponding to the pits. For both EW and LW, the water in the ray cell lumen was included in Peak 3, i.e. water in the ray cell lumina does not seem to give a separate signal from water in the tracheid lumen even for the EW samples. Because of the small relative area under Peak 3, it was not possible to assign this peak differently irrespective of how the dimensions were varied (Table 2).

The results from the ANOVA showed that there was a significant difference between EW and LW in terms of the T_2 values for Peak 2 (Table 6). For the discrete multi-exponential fit, the overall mean T_2 was shorter for the LW specimens. This is logical as the void volumes (bordered pits, lumen), except for those present in ray cells, generally are smaller in LW and would thus give a shorter T_2. From Table 5, it is seen that this shorter T_2 for LW is most pronounced for the extracted specimens. However, for the continuous curve-fit, the T_2 for Peak 2 was generally shorter in case of EW. A comparison between the relative area of Peak 2 and the volume estimations indicates that Peak 2 represents the water in pits. This observation is counterintuitive because the pits are smaller in LW. However, for the continuous fit, Peak 2 was not present for all LW specimens and the mean values are thus based on fewer observations for LW. This is the reason why these results should be interpreted with care.

Correlating the T_2 value with the surface area to volume ratios of the voids would also offer a peak assignment. However, this approach requires that the surface relaxivity is the same throughout the material, which might not be the case due to differences in chemical composition in different parts of the wood structure.

Conclusions

There was a significant difference in T_2 of cell wall water between EW and LW as well as between juvenile and mature wood, but no differences were observable between the sorption isotherms of these anatomical parts of wood. Thus, the reasons for the T_2 differences are not clear, but different chemical cell wall composition or extractive contents are possible explanations. Two peaks corresponding to free water were seen by both the discrete and the continuous curve-fit for both EW and LW. However, when comparing LFNMR signal fractions to estimates of void volumes within the wood structure, the two peaks from the two curve-fit methods do not seem to represent the same water. The free-water peak with the shorter T_2 (Peak 2) constituted a smaller fraction of the total amount of free water for the continuous curve-fit than for the discrete multi-exponential fit, especially in case of LW specimens. For the discrete curve-fit, Peak 2 was assigned to water in the pits and the ray cell lumina, while the free-water peak with the longer T_2 (Peak 3) was assigned to water in the tracheid lumina. However, for the continuous curve-fit, Peak 2 seemed to include only the water in the pits, while the rest of the free water was included in Peak 3. A population with a longer relaxation time than lumen water was found to most likely correspond to water on the specimen's surface.

Acknowledgments: M. Fredriksson acknowledges the funding from the Swedish Research Council Formas. Bengt Nilsson is acknowledged for performing the sorption balance measurements.

References

Almeida, G., Gagné, S., Hernández, R.E. (2007) A NMR study of water distribution in hardwoods at several equlibrium moisture contents. Wood Sci. Technol. 41:293–307.

Araujo, C.D., Mackay, A.L., Hailey, J.R.T., Whittall, K.P., Le, H. (1992) Proton magnetic resonance techniques for characterization of water in wood – application to white spruce. Wood Sci. Technol. 26:101–113.

Araujo, C.D., Avramidis, S., Mackay, A.L. (1994) Behavior of solid wood and bound water as a function of moisture content A proton magnetic resonance study. Holzforschung. 48:69–74.

Back, E. (1958) Aspects on tracheidal and parenchymatous ray cells in pulpwood conifers. Sven. Papperstidn. 17:523–530.

Bertaud, F., Holmbom, B. (2004) Chemical composition of earlywood and latewood in Norway spruce heartwood, sapwood and transition zone wood. Wood Sci. Technol. 38:245–256.

Boutelje, J.B. (1968) Juvenile wood, with particular reference to Northern spruce. Sven. Papperstidn. 17:581–585.

Browning, B.L. The chemistry of wood. John Wiley & Sons, Inc., New York, 1963.

Brownstein, K.R., Tarr, C.E. (1979) Importance of classical diffusion in NMR studies of water in biological cells. Physical Review A. 19:2446–2453.

Brändström, J. (2001) Micro- and ultrastructural aspects of Norway spruce tracheids: a review. IAWA J. 22:333–353.

Elder, T., Houtman, C. (2013) Time-domain NMR study of the drying of hemicellulose extracted aspen (Populus tremuloides Michx.). Holzforschung. 67(4):405–411.

Engelund, E.T., Thygesen, L.G., Hoffmeyer, P. (2010) Water sorption in wood and modified wood at high values of relative humidity. Part 2: Appendix. Theoretical assessment of the amount of capillary water in wood microvoids. Holzforschung. 64:325–330.

Fengel, D., Wegener, G. Wood – Chemistry, Ultrastructure, Reactions. Verlag Kessel, Remagen, Germany 2003.

Flibotte, S., Menon, R.S., MacKay, A.L., Hailey, J.R.T. (1990) Proton magnetic resonance of Western red cedar. Wood Fiber Sci. 22:362–376.

Fredriksson, M., Wadsö, L., Johansson, P., Ulvcrona, T. (2016) Microclimate and moisture content profile measurements in rain exposed Norway spruce (*Picea abies* (L.) Karst.) joints. Wood Mat. Sci. Eng. 11:189–200.

Fukazawa, K., Imagawa, H. (1981) Quantitative analysis of lignin using an UV microscopic image analyser. variation within one growth increment. Wood Sci. Technol. 15:45–55.

Garcia Esteban, L., Simon, C., Garcia Fernandez, F., de Palacios, P., Martin-Sampedro, R., Eugenia Eugenio, M., Hosseinpourpia, R. (2015) Juvenile and mature wood of Abies pinsapo Boissier: sorption and thermodynamic properties. Wood Sci. Technol. 49:725–738.

Gindl, W. (2001) The effect of varying latewood proportion on the radial distribution of lignin content in a pine stem. Holzforschung. 55:455–458.

Hartley, I.D., Kamke, F.A., Peemoeller, H. (1994) Absolute moisture content determination of aspen wood below the fiber saturation point using pulsed NMR. Holzforschung. 48:474–479.

Hartley, I.D., Avramidis, S., MacKay, A.L. (1996) H-NMR studies of water interactions in sitka spruce and western hemlock: Moisture content determination and second moments. Wood Sci. Technol. 30:141–148.

Harwood, V.D. (1971) Variation in carbohydrate analyses in relation to wood age in Pinus radiata. Holzforschung. 25:73–77.

Hill, C., Moore, J., Jalaludin, Z., Leveneu, M., Mahrdt, E. (2011) Influence of earlywood/latewood and ring position upon water vapour sorption properties of Sitka spruce. Int. Wood Prod. J. 2:12–19.

Hsieh, C.-w.C., Cannella, D., Jørgensen, H., Felby, C., Thygesen, L.G. (2014) Cellulase inhibition by high concentrations of monosaccharides. J. Agr. Food Chem. 62:3800–3805.

Ibach, R.E. (2013) Biological properties of wood. In: Handbook of Wood Chemistry and Wood Composites. Ed. Rowell, R.M. CRC Press, Taylor & Francis Group, Boca Raton.

Ilvessalo-Pfäffli, M.S. Fiber atlas – Identification of papermaking fibers. Springer-Verlag, Berlin 1995.

Javed Muhammad, A., Kekkonen Päivi, M., Ahola, S., Telkki, V.-V. (2015) Magnetic resonance imaging study of water absorption in thermally modified pine wood. Holzforschung. 69:899–907.

Kaakinen, S., Saranpää, P., Vapaavuori, E. (2007) Effects of growth differences due to geographic location and N-fertilisation on wood chemistry of Norway spruce. Trees. 21:131–139.

Khattak, T.M., Mahmood, A. (1986) Estimation of lignin, holocellulose and alphacellulose content of earlywood and latewood among innerwood and outerwood of Blue pine (*Pinus wallichiana* A.B. Jacks.) Pak. J. Bot. 18:235–241.

Labbé, N., De Jéso, B., Lartigue, J.C., Daudé, G., Pétraud, M., Ratier, M. (2002) Moisture content and extractive materials in maritime pine wood by low field ^{1}H NMR. Holzforschung. 56:25–31.

Labbé, N., De Jéso, B., Lartigue, J.C., Daudé, G., Pétraud, M., Ratier, M. (2006) Time-domain ^{1}H NMR characterization of the liquid phase in greenwood. Holzforschung. 60:265–270.

McDonald, P.J., Rodin, V., Valori, A. (2010) Characterisation of intra- and inter-C–S–H gel pore water in white cement based on an analysis of NMR signal amplitudes as a function of water content. Cement Concrete Res. 40:1656–1663.

Meier, H. (1962) Chemical and morphological aspects of the fine structure of wood. Pure Appl. Chem. 5:37–52.

Menon, R.S., Mackay, A.L., Hailey, J.R.T., Bloom, M., Burgess, A.E., Swanson, J.S. (1987) An NMR determination of the physiological water distribution in wood during drying. J. Appl. Polym. Sci. 33:1141–1155.

Menon, R.S., Mackay, A.L., Flibotte, S., Hailey, J.R.T. (1989) Quantitative separation of NMR images of water in wood on the basis of T2. J. Magn, Reson. 82:205–210.

Merela, M., Oven, P., Sersa, I., Mikac, U. (2009) A single point NMR method for an instantaneous determination of the moisture content of wood. Holzforschung. 63:348–351.

Nyrén, V., Back, E. (1960) Characteristics of parenchymatic cells and tracheidal ray cells in *Picea abies* Karst. Sven. Papperstidn. 16:501–509.

Pedersen, H.T., Bro, R., Engelsen, S.B. (2002) Towards rapid and unique curve resolution of low-field NMR relaxation data: Trilinear SLICING versus two-dimensional curve fitting. J. Magn. Reson. 157:141–155.

Provencher, S.W. (1982) Contin: A general purpose constrained regularization program for inverting noisy linear algebraic and integral equations. Comput. Phys. Commun. 27:229–242.

Rowell, R., Pettersen, R., Tshabalala (2013) Cell wall chemistry. In: Handbook of Wood Chemistry and Wood Composites. Ed. Rowell, R. Taylor and Francis, Boca Raton.

Rutledge, D.N. (1992) Low resolution pulse nuclear magnetic resonance (LRP-NMR). Analusis Magazine. 20:58–62.

Schweingruber, F.H. Wood Structure and Environment. Springer-Verlag, Berlin, Heidelberg, 2007.

Sharp, A.R., Riggin, M.T., Kaiser, R., Schneider, M.H. (1978) Determination of moisture content of wood by pulsed nuclear magnetic resonance. Wood Fiber. 10:74–81.

Sharratt, V., Hill, C.A.S., Zaihan, J., Kint, D.P.R. (2011) The influence of photodegradation and weathering on the water vapour sorption kinetic behaviour of scots pine earlywood and latewood. Polym. Degred. Stabil. 96:1210–1218.

Shmulsky, R., Jones, P.D. Forest Products and Wood Science: An Introduction, 6th edition. Wiley-Blackwell, Chichester, 2011.

Shupe, T.F., Hse, C.Y., Choong, E.T., Groom, L.H. (1997) Differences in some chemical properties of innerwood and outerwood from five silviculturally different loblolly pine stands. Wood Fiber Sci. 29:91–97.

Siau, J.F. Transport Processes in Wood. Springer-Verlag, Berlin 1984.

Telkki, V.V., Yliniemi, M., Jokisaari, J. (2013) Moisture in softwoods: fiber saturation point, hydroxyl site content, and the amount of micropores as determined from NMR relaxation time distributions. Holzforschung. 67:291–300.

Terenzi, C., Dvinskikh, S.V., Furó, I. (2013) Wood microstructure explored by anisotropic 1H NMR line broadening: experiments and numerical simulations. J Phys Chem B 117:8620–8632.

Terenzi, C., Prakobna, K., Berglund, L.A., Furó, I. (2015) Nanostructural effects on polymer and water dynamics in cellulose biocomposites: 2H and 13C NMR relaxometry. Biomacromolecules 16:1506–1515.

Thygesen, L.G., Elder, T. (2008) Moisture in untreated, acetylated, and furfurylated Norway spruce studied during drying using time domain NMR. Wood Fiber Sci. 40:309–320.

Thygesen, L.G., Elder, T. (2009) Moisture in untreated, acetylated and furfurlated Norway spruce monitored during drying below fiber saturation using time domain NMR. Wood Fiber Sci. 41:194–200.

Timell, T.E. (1965) Wood and bark polysaccharides. In: Cellular Ultrastructure of Woody Plants – Advanced Science Seminar. Ed. Côté, W.A. New York. Syracuse University Press.

Uprichard, J.M. (1971) Cellulose and lignin content in Pinus radiata D. Don. Within tree variation in chemical composition, density and tracheid length. Holzforschung 25:97–105.

Usta, I., Hale, M.D. (2006) Comparison of the bordered pits of two species of spruce (Pinaceae) in a green and kiln-dried condition and their effects on fluid flow in the stem wood in relation to wood preservation. Forestry 79:467–475.

Williams, D.R. (1995) The characterisation of powders by gravimetric water vapour sorption. Int. LABMATE. 20:40–42.